Research Article | Vol. 26, No. 25 | 10 Dec 2018 | OPTICS EXPRESS 32624
Optics EXPRESS

Engineering scattering patterns with asymmetric dielectric nanorods

SUHANDOKO D. ISRO,[1] ALEXANDER A. ISKANDAR,[1,3] YURI S. KIVSHAR,[2] AND ILYA V. SHADRIVOV[2,*]

[1]*Physics of Magnetism and Photonics Research Division, Faculty of Mathematics and Natural Sciences, Institut Teknologi Bandung, Jl. Ganesha 10, Bandung 40132, Indonesia*
[2]*Nonlinear Physics Centre, Research School of Physics and Engineering, Australian National University, ACT 2601, Australia*
[3]*iskandar@fi.itb.ac.id*
[*]*ilya.shadrivov@anu.edu.au*

Abstract: By controlling interference of Mie resonance modes of various nanostructures, we can achieve a large number of nontrivial effects in nanophotonics. In this work, we propose a cylindrical structure in which the spectral overlap of the Mie-type modes can be controlled by drilling a hole parallel to the axis, thus changing unidirectional scattering. We further demonstrate that the scattering patterns can be tailored by rotating the structure to achieve almost arbitrary scattered wave direction.

1. Introduction

In the last decade, researchers have been fascinated by the possibilities of light manipulation using subwavelength structures. In particular, high-index all-dielectric nanostructures were proposed for a range of applications due to their ability to provide strong light-matter interaction [1–5]. In such systems the optical resonance can be tuned by varying the material and geometry parameters of the structure. All-dielectric Mie-resonant nanostructures are now seen as a replacement for plasmonics structures that previously were proposed for various applications, including magnetic field localization and enhancement [6], scattering cancellation [7], light absorption and trapping [8–13].

It has been shown both theoretically [14–19] and experimentally [20–22] that all-dielectric optical nanostructures can support strong electric and magnetic dipolar and multipolar resonances.

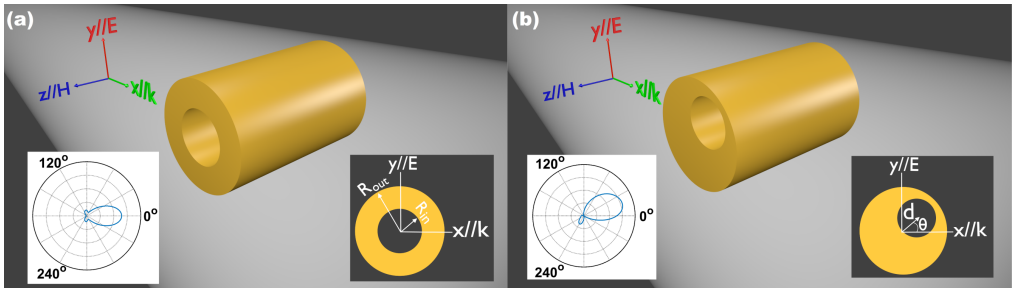

Fig. 1. Schematics of the problem. (a) A hollow nanorod structure with outer radius $R_{out} = 450$ nm and refractive index $\tilde{n} = 3.4 + i\,0.01$. (b) An asymmetric nanorod structure with the same outer radius and refractive index. Both structures are illuminated by TE-polarized plane wave propagating in x-direction as indicated by the colored arrows. The insets in each figure show the cross-sectional view as well as an example of angular intensity distribution for each structure.

#344344 https://doi.org/10.1364/OE.26.032624
Journal © 2018 Received 11 Sep 2018; revised 28 Oct 2018; accepted 29 Oct 2018; published 28 Nov 2018

Optics EXPRESS

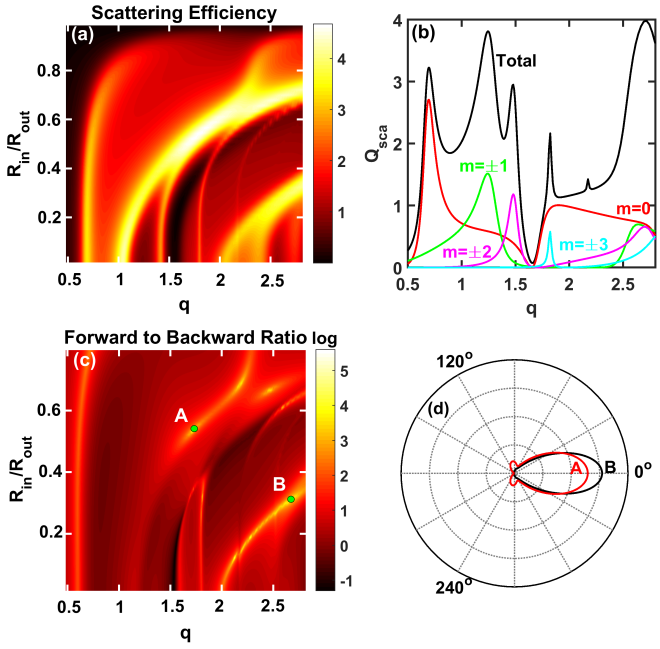

Fig. 2. (a) Scattering efficiency of a symmetric hollow nanorod as a function of the ratio of the inner radius to the outer radius $R_{\text{in}}/R_{\text{out}}$ and size parameter $q = k_0 R_{out}$. (b) Scattering efficiency spectra obtained by taking a horizontal cross-section of Fig. 2(a) at $R_{\text{in}}/R_{\text{out}} = 0.3$ along with the mode decomposition. (c) Ratio of forward scattering (the scattered wave intensity at $\phi = 0^{\text{o}}$) to backward scattering (the scattered wave intensity at $\phi = 180^{\text{o}}$). (d) Angular intensity distributions corresponding to the marked points in Fig. 2(c).

Furthermore, those resonances can occur in overlapping frequency ranges, producing interference and resulting in interesting scattering phenomena [23–28]. One of the most critical outcomes of this interference is the simultaneous excitation of electric dipole mode (ED) and magnetic dipole mode (MD) with balanced strengths which leads to the Kerker condition of zero backward scattering [29–34]. This condition is important in many applications such as nanoantennas [35–37], optical sensing [38], and photovoltaics [39]. Recently, it has been shown that Kerker condition can occur even in a simple homogeneous dielectric nanorod [40,41]. In an infinitely long homogeneous cylinder or in a sphere each Mie resonance mode has a distinct resonance wavelength, thus the interference effects cannot be controlled substantially. To obtain a more desirable interference effects between the ED and MD modes in long cylindrical structures one will usually try to overlap the two resonances by using metal-dielectric composite structures [42–44]. Unfortunately, Kerker condition is by no means a perfect way to achieve directional scattering since the interference of the ED and MD modes produces substantial scattering in other directions [45]. Another way to obtain a more preferable scattering pattern is through the interference of the electric quadrupole mode (EQ) and the electric dipole mode (ED) known as the generalized Kerker condition [46,47] or by interfering higher resonance modes [44, 48, 49].

In this paper, we show that unidirectional scattering patterns can be engineered by using a simple structure of an asymmetric hollow dielectric nanorod. Most structures proposed so far in the field of nanophotonics act only as a passive system which gives almost no flexibility for controlling the beam deflection. Lately, a system of coupled dipole and a sphere was envisaged to overcome that shortcoming [50]. It was also shown that interference of the Mie resonance modes in dielectric metalattices can exhibit the beam deflection effect [51]. Here, we outline the

Optics EXPRESS

possibility of the beam deflection by rotating a hollow asymmetric nanorod.

2. Scattering by a nanorod

Our system consists of an infinitely long hollow nanorod with fixed outer radius R_{out} (in all following calculations we assume $R_{\text{out}} = 450$ nm) and refractive index $\tilde{n} = 3.4 + \text{i}0.01$. The nanorod is illuminated by the transverse electric (TE) plane wave (see Fig. 1) with wavelength λ. First, we discuss the scattering of a symmetric hollow nanorod [Fig. 1(a)] and its dependence on the hole radius. Next, we study the effect of asymmetric hole position in the nanorod [Fig. 1(b)]. We write the general expression for the magnetic field in all regions as follows [52, 53]

$$\mathcal{H}_{z1} = \sum_n [A_{1n}\text{J}_n(k_1\rho_1)]e^{\text{i}n\phi_1}, \tag{1}$$

$$\mathcal{H}_{z2} = \sum_n [A_{2n}\text{J}_n(k_2\rho_1) + B_{2n}\text{H}_n(k_2\rho_1)]e^{\text{i}n\phi_1}, \tag{2}$$

$$\mathcal{H}_{z3} = \sum_m [\text{i}^m\text{J}_m(k_3\rho_2) + B_{3m}\text{H}_m(k_3\rho_2)]e^{\text{i}m\phi_2}, \tag{3}$$

where $\mathcal{H}_{z1}$, $\mathcal{H}_{z2}$ and $\mathcal{H}_{z3}$ are the general expressions for magnetic fields in the hole region, in the dielectric shell and in the surrounding background, respectively. Each solution consists of cylindrical wave representation described by integer order Hankel function of the first kind ($\text{H}_{m/n}(k_\ell\rho_j)$) and Bessel function ($\text{J}_{m/n}(k_\ell\rho_j)$) with $k_\ell = \omega\sqrt{\varepsilon_\ell}/\text{c}$ ($\ell = 1, 2, 3$). The two polar coordinate systems introduced, (ρ_1, ϕ_1) and (ρ_2, ϕ_2), are associated with the two origins located at the hole and shell axes, respectively. Both coordinate systems are related to each other through Graf′s addition theorem as

$$\text{J/H}_n(k_2\rho_1)e^{\text{i}n\phi_1} = \sum_m \text{J}_{m-n}(k_2d)e^{-\text{i}(m-n)\theta}\text{J/H}_m(k_2\rho_2)e^{\text{i}m\phi_2}, \tag{4}$$

in which (d, θ) are the offset parameters representing the relative position of the hole axis with respect to the coordinate system of the rod. The unknown field coefficients A_{1n}, A_{2n}, B_{2n} and B_{3m} can thus be determined from the boundary conditions at the two interfaces. It follows that in this system the scattering efficiency can be written as

$$\text{Q}_{\text{sca}} = \frac{\text{Re}\left[\int(\mathbf{E}_{\text{sca}} \times \mathbf{H}^*_{\text{sca}}) \cdot \hat{\rho}\,\text{d}\phi\right]}{4\text{I}_{\text{inc}}}, \tag{5}$$

where $\mathbf{E}_{\text{sca}}$ denotes the corresponding scattered electric field solutions and I_{inc} is the incoming wave intensity. In general, the integral in Eq. (5) can be calculated numerically for any desired angular limit. Nevertheless, in most cases the integral is calculated over an imaginary closed surface covering the scatterer, thus giving us the standard formula of scattering efficiency

$$\text{Q}_{\text{sca}} = \frac{2}{q}\sum_{m=-\infty}^{\infty}|B_{3m}|^2, \tag{6}$$

in which $|B_{3m}|$ is the amplitude of the scattered wave and $q = k_0R_{\text{out}} = 2\pi\ R_{\text{out}}/\lambda$ is the so-called size parameter. In the case of TE wave illumination, $m = 0$ corresponds to the MD mode, while $m = \pm1$ and $m = \pm2$, respectively, are the ED mode and the EQ mode [48].

Optics EXPRESS

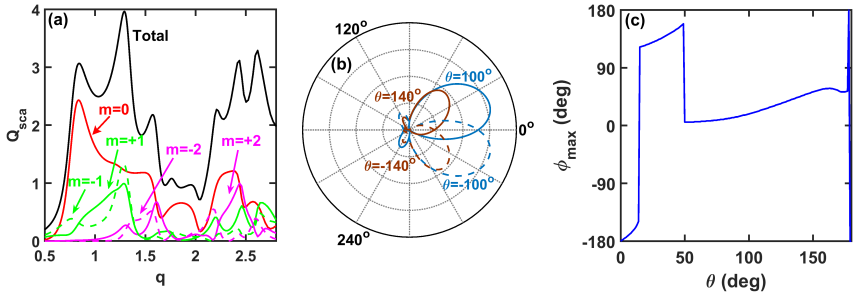

Fig. 3. (a) Scattering efficiency Q_{sca} calculated for the asymmetric nanorod system for $(R_{in}, d, \theta) = (0.5R_{out}, 0.4R_{out}, 100^o)$, (b) Scattering diagrams calculated at $q = 2.24$ for $\theta = 100^o$ (solid blue), 140^o (solid brown), -100^o (dashed blue), -140^o (dashed brown). (c) The angle of the major scattering lobe as a function of the angle θ.

2.1. Symmetric nanorod

In Fig. 2(a) we show the dependence of the scattering efficiency of a hollow nanorod on the ratio of the hole radius to outer radius, with each bright line in the figure corresponding to different resonance modes. We observe that by increasing the ratio of radii we can achieve an overlap of some of the resonances. By taking a horizontal slice of Fig. 2(a) at $R_{in}/R_{out} = 0.3$, we observe several resonances in the scattering cross-section. By plotting the contributions of individual multipoles to the scattering efficiency, we identify their contributions, with magnetic dipole ($m = 0$), electric dipole ($m = \pm 1$) and electric quadrupole mode ($m = \pm 2$) as shown in Fig. 2(b). We notice that, due to the symmetry in this case, the contributions of positive and negative m modes are identical. Each of the modes, individually, possesses various symmetries, however when we overlap the resonances, the ratio of the forward scattering (the scattered wave intensity at $\phi = 0^o$) to backward scattering (the scattered wave intensity at $\phi = 180^o$) can be controlled, as is seen in Fig. 2(c). The enhanced forward scattering is due to the constructive interference in the forward direction, and destructive interference in the backward direction of the ED and EQ modes, as predicted by the generalized Kerker condition [46]. The scattering pattern for the system parameters specified by $(R_{in}/R_{out}, q) = (0.3, 2.618)$ (point B) and $(R_{in}/R_{out}, q) = (0.52, 1.673)$ (point A) are shown in Fig. 2(d). It is clear that the scattering patterns are unidirectional, with enhancement in the forward direction and suppression in the backward direction.

2.2. Beam deflection with asymmetric hollow nanorods

It was shown earlier that the expression of scattering efficiency (Q_{sca}) for the problem of scattering by a hollow cylinder with non-coaxial inner core can still be written in the form of Eq. (6). To see the differences of scattering by a concentric and non-concentric hollow cylinder, we begin by studying the configuration with $(R_{in}, d, \theta) = (0.5R_{out}, 0.4R_{out}, 100^o)$. Here, d is the distance between the hole axis and the nanorod axis, and θ is the angle of the core-offset direction with respect to the direction of the incoming wave [see Fig. 1(b)].

One can see from Fig. 3(a) that the scattering coefficient arising from the positive-m modes is no longer the same as that from the negative modes: $|B_{3(-m)}| \neq |B_{3(+m)}|$. This phenomenon is clearly the result of azimuthal symmetry breaking in the system. Due to this phenomenon, it becomes possible to obtain a more diverse interference effects between the Mie resonance modes. As a demonstration, in Fig. 3(b) we show that the angle of the main scattering lobe can be engineered by simply rotating the nonconcentric hollow nanorod. On the other hand, Fig. 3(c) shows the dependence of the angle of the main lobe of scattering on the angular position of the hole. We see that by rotating the nanorod we can control direction of scattering in a wide range

Optics EXPRESS

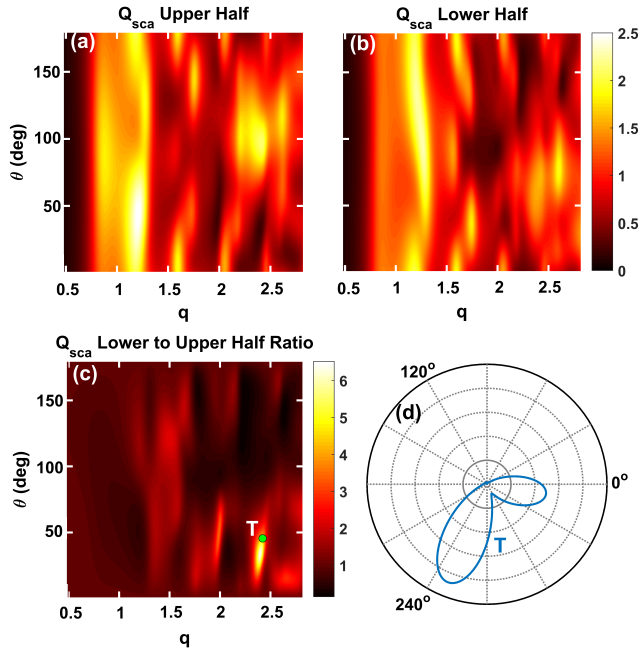

Fig. 4. (a) The scattering efficiency Q_{sca} calculated only for the upper half-space ($y > 0$), (b) the Q_{sca} calculated only for the lower half-space ($y < 0$), (c) The ratio of scattering in the lower half-space to that in upper half-space. (d) The angular intensity distribution for the parameters corresponding to the point T in figure (c). All figures are calculated for asymmetric nanorod structure with $R_{out} = 450$ nm, $R_{in} = 0.5R_{out}$ and $d = 0.4R_{out}$.

of angles, however we cannot cover the whole 2π range.

It follows from Fig. 3 that the angular scattering intensity distribution resulted from an asymmetric nanorod structure is no longer symmetric with respect to the horizontal axis. This condition may lead to an unbalanced total power radiated in the upward direction and in the downward direction, as observed in Fig. 4. In Fig. 4(a) the scattering efficiency is calculated for upper half space, whereas in Fig. 4(b) the calculation is done for the lower half. It is clear that the total power radiated into the two directions is different. By calculating the ratio of the energy flow in the downward direction to that in the upward direction, we find the parameters for which the energy is mostly radiated in the downward direction, as shown in Fig. 4(c). For example, the angular intensity distribution for the point T in Fig. 4(c) is shown in Fig. 4(d), which suggests that the scattering occurs mostly in the downward direction. We note that such an unbalanced radiation will result in a transverse optical force, hence the asymmetric nanorod system can be utilized for controlling the optical force direction [54].

3. Conclusions

We have studied the scattering properties of a hollow dielectric nanorod structure. We have observed that manipulation of the mutual position of various resonances of the structure can be controlled by changing the radius and position of the hole within the nanorod. We have shown that, in general, higher-order resonances are less sensitive to a variation of the hole size, and this can lead to a merging of resonances and their resulting interference. In particular, for the considered structures, the dominating resonances are electric dipole and electric quadrupole, which in the symmetric case produce unidirectional scattering characterized by a pattern with

Optics EXPRESS

zero backward scattering. We have further demonstrated the possibility of the beam deflection by using a hollow nanorod structure with asymmetrically placed hole. Due to the azimuthal symmetry breaking, the scattering amplitude of the modes with positive and negative azimuthal numbers became different, resulting in unconventional scattering patterns. Unbalanced radiation power occurs for the more complex resonances interference which can be useful for tailoring the transverse optical forces.

Funding

Institut Teknologi Bandung (071/I1.B04/SPKWRRIM/III/2017).

Acknowledgments

This work was partially supported by Program Penelitian, Pengabdian Kepada Masyarakat dan Inovasi (P3MI) 2017 from Institut Teknologi Bandung (contract no. 071/I1.B04/SPK-WRRIM/III/2017). I.V.S. and Y.S.K acknowledge support from the Australian Research Council through Discovery Project and Future Fellowship schemes.

References

1. Y. Kivshar and A. Miroshnichenko, "Meta-optics with mie resonances," Opt. Photonics News **28**, 24–31 (2017).
2. A. I. Kuznetsov, A. E. Miroshnichenko, M. L. Brongersma, Y. S. Kivshar, and B. Luk'yanchuk, "Optically resonant dielectric nanostructures," Science **354**, aag2472 (2016).
3. W. Liu, A. E. Miroshnichenko, and Y. S. Kivshar, "Control of light scattering by nanoparticles with optically-induced magnetic responses," Chin. Phys. B **23**, 047806 (2014).
4. J. A. Schuller and M. L. Brongersma, "General properties of dielectric optical antennas," Opt. Express **17**, 24084–24095 (2009).
5. S. Jahani and Z. Jacob, "All-dielectric metamaterials," Nat. Nanotechnol. **11**, 23–36 (2016).
6. K. V. Baryshnikova, A. Novitsky, A. B. Evlyukhin, and A. S. Shalin, "Magnetic field concentration with coaxial silicon nanocylinders in the optical spectral range," J. Opt. Soc. Am. B **34**, D36–D41 (2017).
7. A. Mirzaei, A. E. Miroshnichenko, I. V. Shadrivov, and Y. S. Kivshar, "All-dielectric multilayer cylindrical structures for invisibility cloaking," Sci. Rep. **5** (2015).
8. J. Grandidier, D. M. Callahan, J. N. Munday, and H. A. Atwater, "Light absorption enhancement in thin-film solar cells using whispering gallery modes in dielectric nanospheres," Adv. Mater. **23**, 1272–1276 (2011).
9. A. Raman, Z. Yu, and S. Fan, "Dielectric nanostructures for broadband light trapping in organic solar cells," Opt. Express **19**, 19015–19026 (2011).
10. S. A. Mann, R. R. Grote, R. M. Osgood, and J. A. Schuller, "Dielectric particle and void resonators for thin film solar cell textures," Opt. Express **19**, 25729–25740 (2011).
11. A. P. Vasudev, J. A. Schuller, and M. L. Brongersma, "Nanophotonic light trapping with patterned transparent conductive oxides," Opt. Express **20**, A385–A394 (2012).
12. C. van Lare, F. Lenzmann, M. A. Verschuuren, and A. Polman, "Dielectric scattering patterns for efficient light trapping in thin-film solar cells," Nano Lett. **15**, 4846–4852 (2015).
13. L. Cao, J. S. White, J.-S. Park, J. A. Schuller, B. M. Clemens, and M. L. Brongersma, "Engineering light absorption in semiconductor nanowire devices," Nat. Mater. **8**, 643–647 (2009).
14. A. Ahmadi and H. Mosallaei, "Physical configuration and performance modeling of all-dielectric metamaterials," Phys. Rev. B **77**, 045104 (2008).
15. A. B. Evlyukhin, C. Reinhardt, A. Seidel, B. S. Luk'yanchuk, and B. N. Chichkov, "Optical response features of si-nanoparticle arrays," Phys. Rev. B **82**, 045404 (2010).
16. A. B. Evlyukhin, C. Reinhardt, and B. N. Chichkov, "Multipole light scattering by nonspherical nanoparticles in the discrete dipole approximation," Phys. Rev. B **84**, 235429 (2011).
17. A. García-Etxarri, R. Gómez-Medina, L. S. Froufe-Pérez, C. López, L. Chantada, F. Scheffold, J. Aizpurua, M. Nieto-Vesperinas, and J. J. Sáenz, "Strong magnetic response of submicron silicon particles in the infrared," Opt. Express **19**, 4815–4826 (2011).
18. J. Van de Groep and A. Polman, "Designing dielectric resonators on substrates: Combining magnetic and electric resonances," Opt. Express **21**, 26285–26302 (2013).
19. M. A. van de Haar, J. van de Groep, B. J. Brenny, and A. Polman, "Controlling magnetic and electric dipole modes in hollow silicon nanocylinders," Opt. Express **24**, 2047–2064 (2016).
20. J. A. Schuller, R. Zia, T. Taubner, and M. L. Brongersma, "Dielectric metamaterials based on electric and magnetic resonances of silicon carbide particles," Phys. Rev. Lett. **99**, 107401 (2007).
21. A. I. Kuznetsov, A. E. Miroshnichenko, Y. H. Fu, J. Zhang, and B. LukâĂŹYanchuk, "Magnetic light," Sci. Rep. **2**, 492 (2012).

Optics EXPRESS

22. A. B. Evlyukhin, R. L. Eriksen, W. Cheng, J. Beermann, C. Reinhardt, A. Petrov, S. Prorok, M. Eich, B. N. Chichkov, and S. I. Bozhevolnyi, "Optical spectroscopy of single si nanocylinders with magnetic and electric resonances," Sci. Rep. **4**, 4126 (2014).
23. S. Person, M. Jain, Z. Lapin, J. J. Sáenz, G. Wicks, and L. Novotny, "Demonstration of zero optical backscattering from single nanoparticles," Nano Lett. **13**, 1806–1809 (2013).
24. I. Staude, A. E. Miroshnichenko, M. Decker, N. T. Fofang, S. Liu, E. Gonzales, J. Dominguez, T. S. Luk, D. N. Neshev, I. Brener, and Y. Kivshar, "Tailoring directional scattering through magnetic and electric resonances in subwavelength silicon nanodisks," ACS Nano **7**, 7824–7832 (2013).
25. M. Nieto-Vesperinas, R. Gomez-Medina, and J. Saenz, "Angle-suppressed scattering and optical forces on submicrometer dielectric particles," J. Opt. Soc. Am. A **28**, 54–60 (2011).
26. Y. H. Fu, A. I. Kuznetsov, A. E. Miroshnichenko, Y. F. Yu, and B. Luk'yanchuk, "Directional visible light scattering by silicon nanoparticles," Nat. Commun. **4**, 1527 (2013).
27. D. A. Powell, "Interference between the modes of an all-dielectric meta-atom," Phys. Rev. Appl. **7**, 034006 (2017).
28. M. I. Tribelsky, J.-M. Geffrin, A. Litman, C. Eyraud, and F. Moreno, "Small dielectric spheres with high refractive index as new multifunctional elements for optical devices," Sci. Rep. **5** (2015).
29. M. Kerker, D.-S. Wang, and C. Giles, "Electromagnetic scattering by magnetic spheres," JOSA **73**, 765–767 (1983).
30. R. Alaee, M. Albooyeh, M. Yazdi, N. Komjani, C. Simovski, F. Lederer, and C. Rockstuhl, "Magnetoelectric coupling in nonidentical plasmonic nanoparticles: Theory and applications," Phys. Rev. B **91**, 115119 (2015).
31. X. Zambrana-Puyalto, I. Fernandez-Corbaton, M. Juan, X. Vidal, and G. Molina-Terriza, "Duality symmetry and kerker conditions," Opt. Lett. **38**, 1857–1859 (2013).
32. B. Rolly, B. Stout, and N. Bonod, "Boosting the directivity of optical antennas with magnetic and electric dipolar resonant particles," Opt. Express **20**, 20376–20386 (2012).
33. S. D. Campbell and R. W. Ziolkowski, "Simultaneous excitation of electric and magnetic dipole modes in a resonant core-shell particle at infrared frequencies to achieve minimal backscattering," IEEE J. Sel. Top. Quantum Electron. **19**, 4700209–4700209 (2013).
34. W. Liu and Y. S. Kivshar, "Generalized kerker effects in nanophotonics and meta-optics," Opt. Express **26**, 13085–13105 (2018).
35. L. Novotny and N. Van Hulst, "Antennas for light," Nat. Photonics **5**, 83–90 (2011).
36. A. G. Curto, G. Volpe, T. H. Taminiau, M. P. Kreuzer, R. Quidant, and N. F. van Hulst, "Unidirectional emission of a quantum dot coupled to a nanoantenna," Science **329**, 930–933 (2010).
37. L. Zou, W. Withayachumnankul, C. M. Shah, A. Mitchell, M. Bhaskaran, S. Sriram, and C. Fumeaux, "Dielectric resonator nanoantennas at visible frequencies," Opt. Express **21**, 1344–1352 (2013).
38. A. Kabashin, P. Evans, S. Pastkovsky, W. Hendren, G. Wurtz, R. Atkinson, R. Pollard, V. Podolskiy, and A. Zayats, "Plasmonic nanorod metamaterials for biosensing," Nat. Mater. **8**, 867–871 (2009).
39. H. A. Atwater and A. Polman, "Plasmonics for improved photovoltaic devices," Nat. Mater. **9**, 205–213 (2010).
40. P. R. Wiecha, A. Cuche, A. Arbouet, C. Girard, G. C. d. Francs, A. Lecestre, G. Larrieu, F. Fournel, V. Larrey, T. Baron, and V. Paillard, "Strongly directional scattering from dielectric nanowires," ACS Photonics **4**, 2036–2046 (2017).
41. A. F. Cihan, A. G. Curto, S. Raza, P. G. Kik, and M. L. Brongersma, "Silicon mie resonators for highly directional light emission from monolayer mos 2," Nat. Photonics **12**, 284 (2018).
42. E. Rusak, I. Staude, M. Decker, J. Sautter, A. E. Miroshnichenko, D. A. Powell, D. N. Neshev, and Y. S. Kivshar, "Hybrid nanoantennas for directional emission enhancement," Appl. Phys. Lett. **105**, 221109 (2014).
43. W. Liu, A. E. Miroshnichenko, D. N. Neshev, and Y. S. Kivshar, "Broadband unidirectional scattering by magnetoelectric core–shell nanoparticles," ACS Nano **6**, 5489–5497 (2012).
44. W. Liu, J. Zhang, B. Lei, H. Ma, W. Xie, and H. Hu, "Ultra-directional forward scattering by individual core-shell nanoparticles," Opt. Express **22**, 16178–16187 (2014).
45. W. Liu, A. E. Miroshnichenko, R. F. Oulton, D. N. Neshev, O. Hess, and Y. S. Kivshar, "Scattering of core-shell nanowires with the interference of electric and magnetic resonances," Opt. Lett. **38**, 2621–2624 (2013).
46. R. Alaee, R. Filter, D. Lehr, F. Lederer, and C. Rockstuhl, "A generalized kerker condition for highly directive nanoantennas," Opt. Lett. **40**, 2645–2648 (2015).
47. I. M. Hancu, A. G. Curto, M. Castro-López, M. Kuttge, and N. F. van Hulst, "Multipolar interference for directed light emission," Nano Lett. **14**, 166–171 (2013).
48. W. Liu, "Superscattering pattern shaping for radially anisotropic nanowires," Phys. Rev. A **96**, 023854 (2017).
49. R. R. Naraghi, S. Sukhov, and A. Dogariu, "Directional control of scattering by all-dielectric core-shell spheres," Opt. Lett. **40**, 585–588 (2015).
50. A. E. Krasnok, D. S. Filonov, C. R. Simovski, Y. S. Kivshar, and P. A. Belov, "Experimental demonstration of superdirective dielectric antenna," Appl. Phys. Lett. **104**, 133502 (2014).
51. W. Liu and A. E. Miroshnichenko, "Beam steering with dielectric metalattices," ACS Photonics **5**, 1733–1741 (2017).
52. H. Yousif and A. Elsherbeni, "Oblique incidence scattering from two eccentric cylinders," J. Electromagn. Waves Appl. **11**, 1273–1288 (1997).
53. C. A. Valagiannopoulos, "Electromagnetic scattering from two eccentric metamaterial cylinders with frequency-dependent permittivities differing slightly each other," PIER **3**, 23–34 (2008).
54. S. Wang and C. Chan, "Lateral optical force on chiral particles near a surface," Nat. Commun. **5**, 4307 (2014).